

Electronic Supplementary Material (ESI)

Engineering of Stilbazolium/iodocuprate Hybrids with Photo/electrical Performances by Modulating Inter- molecular Charge Transfers among H-Aggregated Chromophores

Wei Wu, Xiang-Ling Lin, Qian Liu, Yan He, You-Ren Huang, Bin Chen, Hao-Hong
Li*, Zhi-Rong Chen*

Supporting information

Synthesis of Stilbazolium-type Dyes

Synthesis of Stilbazolium/iodocuprate Hybrids

Film Preparations and Photocurrent Response Tests

Cyclic Voltammetry Measurements

Table Caption:

Table S1 Crystal data and structure refinement for 1-3

Table S2 Selected bond lengths (Å) of 1-3

Table S3 Hydrogen bridging details of 1-3

Table S4 π - π stacking interactions in this work (lengths in Å and angles in °)

Table S5 Energy levels of 1-3 calculated from CV results

Figure Caption:

Scheme S1 The preparing process of ITO/active layer/PMMA/Ag memory devices

Fig. S1 ¹H NMR spectra of CMAMP·I (a), HMAMP·I (b) and HMAHP·I (c)

Fig. S2 The 2-D cationic layer of 1 (hydrogen atoms without involved in hydrogen bonds were omitted for clarity)

Fig. S3 XRD patterns of 1(a), 2(b) and 3 (c)

Fig. S4 HOMO (left) and LUMO (right) of CMAMP⁺ dimmer in 1 (a), HMAMP⁺ dimmer in 2 (b) and HMAHP⁺ dimmer in 3 (c)

Fig. S5 *I-V* characteristics curves of ITO/hybrid 3/Ag device

Fig. S6 Band structure of 1

Fig. S7 CV measurements on 1 (a), 2 (b) and 3 (c)

Synthesis of Stilbazolium-type Chromophores

Synthesis of CMAMP·I: 2-picoline (9.87 mL, 0.1 mol) and iodomethane (7.47 mL, 0.12 mol) were refluxed for 12 h in 20 mL ethanol solvent with pale yellow 1,2-dimethylpyridin-1-ium iodide obtained, then it was cooled to room-temperature and filtered, afterwards, the product was washed for several times with ethyl ether and dried in air. 4-[(2-cyanoethyl)-methylamino]-benzaldehyde (3.7600 g, 20 mmol) was added into 20 mL the ethanol suspension containing 4.70 g (20 mmol) 1,2-dimethylpyridin-1-ium iodide in the presence of piperidine (5 drops) as a catalyst. The solution was continued refluxing for 24 h to get orange products and then products was filtered and washed by cold ethanol and dichloromethane for three times. IR (cm⁻¹): 3076(w), 3000(w), 2249(w), 1630(w), 1590(s), 1562(s), 1522(s), 1462(m), 1384(m), 1364(m), 1320(m), 1302(w), 1280(s), 1227(m), 1172(s), 1117(m), 1039(w), 1000(w), 958(m), 844(w), 814(s), 787(w), 772(s), 736(w), 632(w), 574(w), 535(m), 514(w), 431(m). ¹H NMR (400 MHz, DMSO-*d*₆) δ 8.76 (d, 1H), 8.45 (d, *J* = 8.1 Hz, 1H), 8.36 (t, *J* = 7.3 Hz, 1H), 7.91 (d, *J* = 15.7 Hz, 1H), 7.72 (d, 3H), 7.27 (d, *J* = 15.4 Hz, 1H), 6.88 (d, *J* = 7.9 Hz, 2H), 4.30 (s, 3H), 3.79 (s, 2H), 3.06 (s, 3H), 2.78 (s, 2H)

Synthesis of HMAMP·I: The synthesis details were similar to that of CMAMP·I except that 4-[(2-cyanoethyl)-methylamino]-benzaldehyde was replaced with 4-[(2-hydroxyethyl)-methylamino]-benzaldehyde (3.58 g, 20 mmol). IR (cm⁻¹): 3354(s), 3013(w), 2917(w), 1627(m), 1584(s), 1555(s), 1523(s), 1505(s), 1454(s), 1385(s), 1349(w), 1320(s), 1273(s), 1222(w), 1184(m), 1168(s), 1121(m), 1063(m), 1048(m), 998(w), 972(m), 955(w), 910(w), 835(m), 807(s), 769(s), 711(w), 557(w), 533(m), 503(w), 474(w), 430(m). ¹H NMR (400 MHz, DMSO-*d*₆) δ 8.74 (d, *J* = 5.8 Hz, 1H), 8.44 (d, *J* = 8.2 Hz, 1H), 8.33 (t, *J* = 7.6 Hz, 1H), 7.91 (d, *J* = 15.6 Hz, 1H), 7.69 (d, *J* = 8.1 Hz, 3H), 7.21 (d, *J* = 15.8 Hz, 1H), 6.80 (d, *J* = 8.2 Hz, 2H), 4.74 (s, 1H), 4.28 (s, 3H), 3.66 – 3.54 (m, 2H), 3.54 – 3.43 (m, 2H), 3.04 (s, 3H).

Synthesis of HMAHP·I: The synthesis details were similar to that of CMAMP·I except that iodomethane was replaced with 2-iodoethanol (9.35 mL, 0.12 mol), which is refluxing for 24 h and 4-[(2-cyanoethyl)-methylamino]-benzaldehyde was replaced with 4-[(2-hydroxyethyl)-methylamino]-benzaldehyde (3.58 g, 20 mmol). And the solvent was replaced with acetonitrile. IR

(cm⁻¹): 3372(m), 3315(m), 3066(w), 2856(w), 1626(m), 1587(s), 1555(s), 1522(s), 1501(m), 1471(m), 1433(s), 1386(s), 1360(w), 1329(s), 1286(m), 1271(w), 1238(m), 1184(s), 852(w), 1160(s), 1123(m), 1058(s), 1045(s), 999(m), 954(m), 938(w), 885(w), 865(w), 814(s), 805(s), 764(s), 712(m), 604(w), 581(w), 531(s), 475(m), 456(m). ¹H NMR (400 MHz, DMSO-*d*₆) δ 8.65 (d, *J* = 5.1 Hz, 1H), 8.46 (d, *J* = 8.0 Hz, 1H), 8.35 (t, *J* = 7.5 Hz, 1H), 7.89 (d, *J* = 15.4 Hz, 1H), 7.75 – 7.64 (m, 3H), 7.29 (d, *J* = 15.7 Hz, 1H), 6.79 (d, *J* = 7.9 Hz, 2H), 5.18 (s, 1H), 4.80 (s, 2H), 4.72 (s, 1H), 3.84 (s, 2H), 3.58 (s, 2H), 3.51 (s, 2H), 3.04 (s, 3H).

Synthesis of Stilbazolium/iodocuprate Hybrids

(CMAMP)₂(CuI₃)(Acetone)_{0.5} (1): **1** was prepared by the solvothermal method. CMAMP·I (0.0310 g, 0.076 mmol), CuI (0.0313 g, 0.16 mmol) and KI (0.033 g, 0.2 mmol) were dissolved in 10 mL acetone. After stirring at room temperature for 1 h, it was transferred to 20 mL Teflon-lined stainless container, which was heated at 100 °C for 2 d and then slowly cooled to room temperature in 2 d. After being filtered and dried at room temperature, the red rhombic crystals were obtained. Yield: 26.5 % (0.0207 g, based on CMAMP·I). Anal. Cald. for C_{37.5}H₄₃CuI₃N₆O_{0.5} (1030.02): calcd. C 43.73, H 4.21, N 8.16%; found C 43.55, H 4.06, N 7.99%. IR (cm⁻¹): 3056(w), 2905(w), 2243(w), 1704(w), 1629(w), 1589(m), 1559(m), 1522(m), 1504(m), 1458(m), 1437(w), 1381(m), 1362(m), 1320(m), 1281(m), 1228(w), 1188(s), 1170(s), 1119(m), 1043(w), 998(w), 957(s), 816(s), 770(s), 734(w), 539(m), 511(w), 430(m).

[(HMAMP)(Cu₃I₄)]_n (2): The synthesis procedure of **2** was similar to that of **1**, except that the type and amount of starting materials are different: HMAMP·I (0.03 g, 0.076 mmol), CuI (0.028 g, 0.147 mmol) and KI (0.0330 g, 0.2 mmol) in 10 mL methanol. Red plate crystals were obtained with yield of 20.3 % (0.0096 g, based on Cu). Anal. Cald. for C₁₇H₂₁Cu₃I₄N₂O (967.58): calcd. C 21.10, H 2.19, N 2.89%; found C 20.42, H 2.05, N 2.59%. IR (cm⁻¹): 3492(w), 3059(w), 2882(w), 1629(m), 1587(s), 1556(s), 1519(s), 1450(s), 1432(s), 1408(w), 1378(s), 1324(s), 1281(s), 1228(m), 1184(s), 1171(s), 1068(w), 1029(s), 962(s), 939(m), 838(w), 815(s), 802(m), 785(w), 757(s), 739(w), 731(w), 543(m), 535(m), 517(w), 506(w), 479(w), 428(m).

[(HMAHP)₂(Cu₅I₇)]_n (3): **3** was prepared under the same conditions with that of **2** using HMAHP·I as starting material: HMAHP·I (0.04 g, 0.094 mmol), CuI (0.038 g, 0.2 mmol) and KI (0.033 g, 0.2 mmol) in 10 mL. Red plate crystals can be collected with yield: 18.5 % (0.0133 g, based on Cu). Anal. Cald. for C₃₆H₄₆Cu₅I₇N₄O₄ (1804.77): calcd. C 23.96, H 2.57, N 3.10%;

found C 23.75, H 2.34, N 2.98 %. IR (cm⁻¹): 3299(w), 3071(w), 2911(w), 1625(m), 1586(s), 1555(s), 1521(s), 1500(m), 1459(w), 1440(w), 1383(m), 1354(w), 1321(m), 1285(m), 1182(s), 1159(s), 1104(w), 1056(m), 1034(s), 998(w), 958(m), 856(w), 810(s), 758(m), 708(w), 635(w), 580(w), 531(s), 473(s), 412(w).

Film Preparations and Photocurrent Response Tests

The working electrodes were prepared on 0.6×0.6 cm² ITO glasses (pre-cleaned by ethanol, acetone and water) with the scotch tape. The 5 mg samples were dispersed in 1 mL DMF by sonication method. The slurry was spread onto pretreated ITO glass. After air-drying, the working electrodes were further dried at 343 K for 1 h to improve adhesion. Then, the other sides of electrodes were uncoated in order to connect the three-electrode system. All the photo/electrochemical measurements were carried out in 0.2 M Na₂SO₄ aqueous solution, the previously prepared ITO glasses were used as the working electrodes, and Ag/AgCl electrodes were treated as counter/reference electrodes, which was irradiated by simulated solar light (150 W high pressure xenon lamp). The whole experiment is under a dark box. And the photo-irradiation time was 300 s, during which a shutter was placed to cut out the light with interval of 10 s.

Cyclic Voltammetry Measurements

Cyclic voltammetry (CV) was performed with a CHI660E Electrochemical Workstation (Shanghai Chenhua Instruments, China), by use of a typical three-electrode cell. Hybrid films coated on a square FTO glass (working electrode) were scanned anodically and cathodically at a sweeping rate of 0.1 V/s, in an electrolyte solution of 0.1 M tetrabutylammonium hexafluorophosphate (Bu₄⁺PF₆⁻) in dry DCM and THF for oxidation and reduction process, respectively. All electrochemical experiments were carried out under a nitrogen atmosphere at room temperature with a platinum sheet and a silver/silver nitrate (Ag/Ag⁺) reference electrode as the counter electrode and the reference electrode, respectively. According to the redox onset potentials of the CV measurements, the HOMO/LUMO energy levels of the materials are estimated based on the reference energy level of ferrocene (4.8 eV below the vacuum) by using the formula, $E_{\text{HOMO}} = -(eE_{\text{ox onset}} - E_{\text{ox Fc/Fc}^{++}} + 4.8)$ and $E_{\text{LUMO}} = -(eE_{\text{red onset}} - E_{\text{red Fc/Fc}^{++}} + 4.8)$, in which $E_{\text{ox Fc/Fc}^{++}} = 0.12\text{V}$ and $E_{\text{red Fc/Fc}^{++}} = 0.36\text{V}$.

Calculated Method using G09

The π - π stacking interaction strengths were quantified by theoretical calculation using G09

program.¹ Stilbazolium monomers and dimers constructed from cif files were calculated without geometry optimizations. And the stacking interaction energies were defined as $E_{\text{stacking}} = 2 \times E_{\text{moner}} - E_{\text{dimer}}$. During the DFT calculations, B3LYP/6-31g(d) level was applied on C, N, O and H atoms.

Table S1 Crystal data and structure refinement for 1-3

Compound	1	2	3
Empirical formula	C ₇₅ H ₈₆ Cu ₂ I ₆ N ₁₂ O	C ₁₇ H ₂₁ Cu ₃ I ₄ N ₂ O	C ₃₆ H ₄₆ Cu ₅ I ₇ N ₄ O ₄
Formula weight	2060.06	967.58	1804.77
Crystal system	Triclinic	Orthorhombic	Triclinic
Space group	<i>P</i> -1	<i>Pbca</i>	<i>P</i> -1
<i>a</i> /Å	11.4311(8)	7.749(3)	7.75790(10)
<i>b</i> /Å	12.7612(10)	23.701(9)	13.3539(2)
<i>c</i> /Å	13.7276(10)	25.770(9)	23.2205(3)
α /°	86.6270(10)	90	100.7150(10)
β /°	83.697(2)	90	95.0080(10)
γ /°	82.2020(10)	90	101.2030(10)
Volume/Å ³	1970.0(3)	4733(3)	2299.53(6)
<i>Z</i>	1	8	2
<i>D_c</i> /mg·m ⁻³	1.737	2.716	2.607
μ /mm ⁻¹]	2.940	7.900	37.910
F(000)	1004	3552	1676
Reflections, total	13107	42190	28927
Reflections, unique	7512[R(int) = 0.0197]	5414 [R(int) = 0.0366]	10279 [R(int) = 0.0527]
Reflections, observed	6833	4387	8623
Goodness-of-fit on F ²	1.057	1.029	1.075
No. of parameters refined	457	247	509
R indices/ <i>I</i> >2sigma(<i>I</i>)	<i>R</i> ₁ =0.0262, <i>wR</i> ₂ =0.0651	<i>R</i> ₁ = 0.0303, <i>wR</i> ₂ = 0.0753	<i>R</i> ₁ = 0.0431, <i>wR</i> ₂ = 0.1045
Residual extremes(e/Å ³)	0.941/-0.946	1.978/ -1.568	1.647 and -1.760

Table S2 Selected bond lengths (Å) of 1-3

1					
Cu(1)-I(1)	2.5551(5)	Cu(1)-I(2)	2.5546(5)	Cu(1)-I(3)	2.5316(4)
2					
Cu(1)-I(1)#1	2.7253(11)	Cu(1)-I(2)	2.6792(11)	Cu(1)-I(3)	2.6426(11)
Cu(1)-I(4)#1	2.7099(12)	Cu(2)-I(1)	2.7059(11)	Cu(2)-I(2)	2.7233(12)
Cu(2)-I(3)	2.6266(10)	Cu(2)-I(4)#2	2.7213(12)	Cu(3)-I(1)	2.6761(11)
Cu(3)-I(1)#1	2.7088(11)	Cu(3)-I(2)	2.5916(11)	Cu(3)-I(4)	2.6212(12)
Cu(1)-Cu(2)	2.9347(17)	Cu(1)-Cu(3)#1	2.9615(15)	Cu(1)-Cu(3)	2.9668(14)

Cu(2)-Cu(3)#2	2.7677(14)	Cu(2)-Cu(3)	2.9550(14)		
Symmetry codes: #1 x-1/2,y,-z+1/2; #2 x+1/2,y,-z+1/2					
3					
Cu(1)-I(1)	2.6302(12)	Cu(1)-I(2)	2.6597(13)	Cu(1)-I(3)	2.6420(13)
Cu(1)-I(7)#1	2.6487(12)	Cu(2)-I(1)	2.6348(13)	Cu(2)-I(2)	2.6888(13)
Cu(2)-I(4)	2.6475(14)	Cu(2)-I(6)	2.7100(13)	Cu(3)-I(2)#2	2.7145(13)
Cu(3)-I(4)	2.6171(13)	Cu(3)-I(6)	2.7828(14)	Cu(3)-I(7)	2.6348(13)
Cu(4)-I(3)#2	2.6573(13)	Cu(4)-I(5)	2.6301(13)	Cu(4)-I(6)	2.7523(13)
Cu(4)-I(7)	2.6367(13)	Cu(5)-I(1)	2.6390(13)	Cu(5)-I(3)	2.6713(13)
Cu(5)-I(5)	2.6173(12)	Cu(5)-I(6)	2.7842(13)	Cu(1)-Cu(2)	2.8533(17)
Cu(1)-Cu(3)#1	2.7073(16)	Cu(1)-Cu(4)#1	2.7610(17)	Cu(1)-Cu(5)	2.7070(16)
Cu(2)-Cu(5)	2.8172(18)	Cu(3)-Cu(4)	2.7735(18)		
Symmetry codes: #1 x+1,y,z; #2 x-1,y,z					

Table S3 Hydrogen bridging details of 1-3

Compound	D-H...A	D-H/Å	H...A/Å	D...A/Å	∠(D-H...A)°	Symmetry codes
1	C(2)-H(2)···I(1)	0.93	3.00	3.859(3)	154	
	C(3)-H(3)···N(3)	0.93	2.51	3.410(4)	164	1+x,y,-1+z
	C(19)-H(19A)···O(1)	0.96	2.57	3.433(8)	150	-x,1-y,1-z
	C(20)-H(20)···N(3)	0.93	2.52	3.408(5)	161	
	C(21)-H(21)···N(6)	0.93	2.55	3.382(5)	150	-1+x,y,1+z
2	O(1)-H(1)···I(3)	0.82	2.91	3.713(5)	168	3/2-x,1/2+y,z
	C(1)-H(1C)···O(1)	0.96	2.55	3.481(7)	163	x,3/2-y,1/2+z
	C(2)-H(2)···O(1)	0.93	2.54	3.423(7)	158	x,3/2-y,1/2+z
3	O(1)-H(1)···O(1)	0.82	2.44	2.721(10)	101	-x,-y,1-z
	O(2)-H(2)···O(1)	0.82	1.88	2.665(10)	159	x,1+y,z
	O(4)-H(4A)···I(2)	0.82	2.98	3.617(7)	136	
	C(14)-H(14)···I(4)	0.93	3.04	3.881(9)	151	
	C(21)-H(21)···O(4)	0.93	2.48	3.209(11)	136	1-x,2-y,-z

Table S4 π-π stacking interactions in this work (lengths in Å and angles in °)

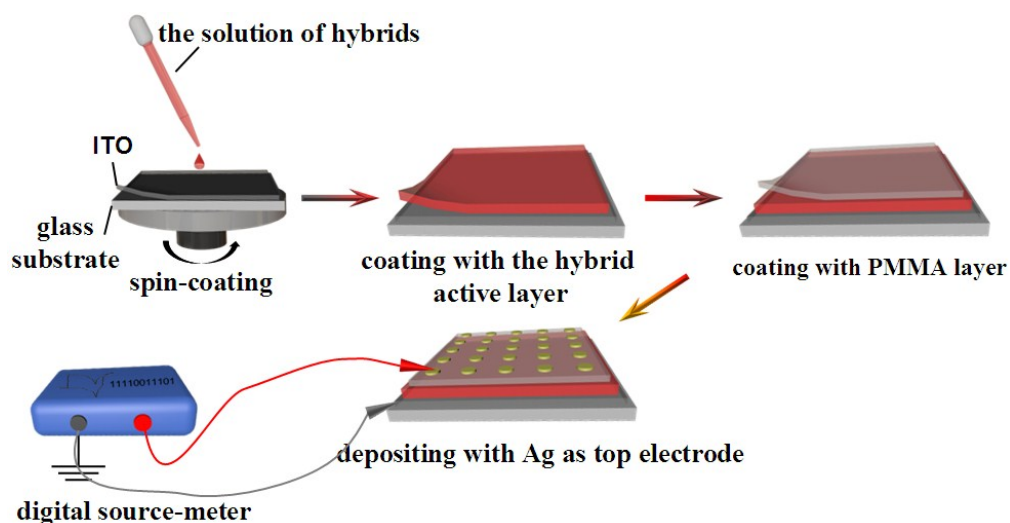
Compound	Cg(I)···Cg(J)	Symmetry code	Dist. Centroids	Dihedral angle	CgI_Perp	CgJ_Perp
1	Cg(1)→Cg(2)	1-x,2-y,1-z	3.5806(18)	2.21(14)	3.4212(13)	3.4561(12)
	Cg(3)→Cg(4)	-x,1-y,1-z	3.4390(17)	1.43(15)	3.3398(13)	3.3390(12)
	Ring(1):N(1)→C(2)→C(3)→C(4)→C(5)→C(6)→; Ring(2): C(9)→C(10)→C(11)→C(12)→C(13)→C(14)→ Ring(3):N(4)→C(20)→C(21)→C(22)→C(23)→C(24)→; Ring(4):C(27)→C(28)→C(29)→C(30)→C(31)→C(32)→					
2	Cg(1)→Cg(2)	1/2+x,y,1/2-z	3.802(4)	9.9(3)	3.597(3)	3.672(2)
	Ring(1):N(1)→C(2)→C(3)→C(4)→C(5)→C(6)→; Ring(2): C(9)→C(10)→C(11)→C(12)→C(13)→C(14)→					
3	Cg(1)→Cg(2)	1-x,1-y,1-z	3.819(5)	1.7(4)	3.460(4)	3.476(4)
	Cg(3)→Cg(4)	2-x,2-y,-z	3.647(5)	3.8(4)	3.319(3)	3.334(3)
	Ring(1):N(1)→C(3)→C(4)→C(5)→C(6)→C(7)→; Ring(2): C(10)→C(11)→C(12)→C(13)→C(14)→C(15)→ Ring(3):N(3)→C(21)→C(22)→C(23)→C(24)→C(25)→; Ring(4):C(28)→C(29)→C(30)→C(31)→C(32)→C(33)→					

Table S5 C-H···π interactions in 3 (distances in Å and angles in °)

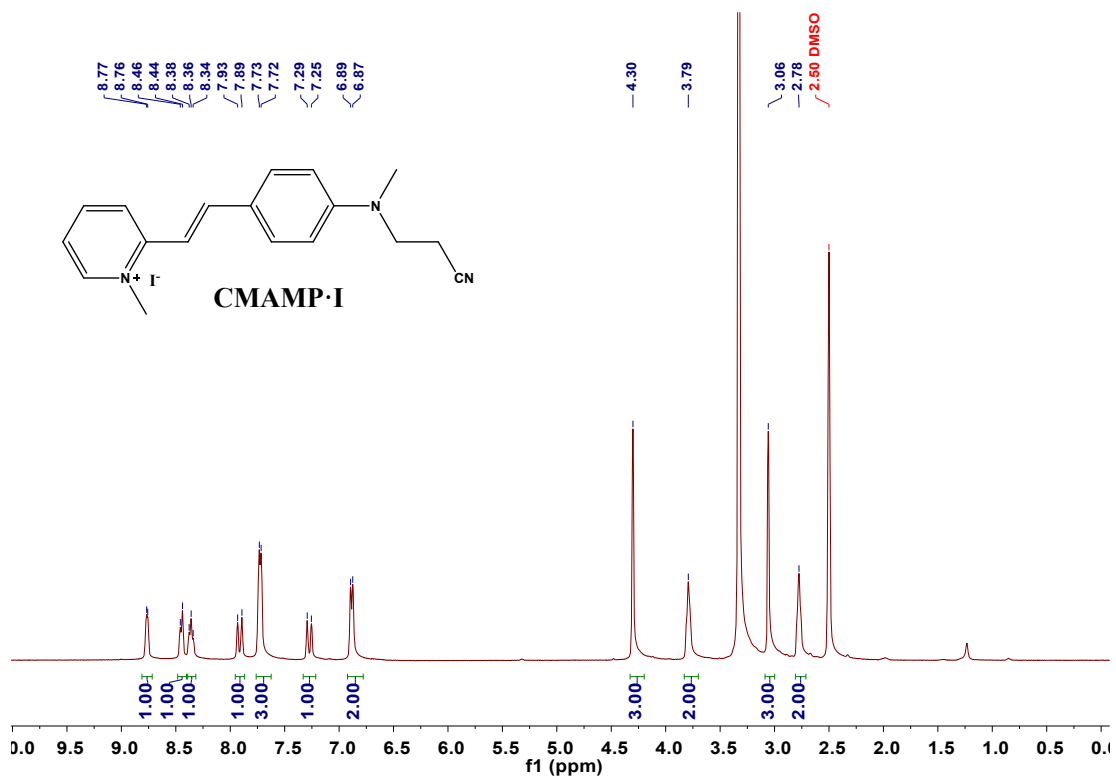
C-H $\cdots\pi$	Distances of H \cdots Cg	Distances of C \cdots Cg	Symmetry code	Angles between Cg-H vector and ring normal	C-H-Cg angles
C(2)-H(2A) \cdots Cg(1)	2.95	3.306(10)	-x,1-y,1-z	17.05	103
Ring(1): C(10) \rightarrow C(11) \rightarrow C(12) \rightarrow C(13) \rightarrow C(14) \rightarrow C(15) \rightarrow					
C(2)-H(2B) \cdots Cg(1)	2.97	3.306(10)	-x,1-y,1-z	16.75	101
Ring(1): C(10) \rightarrow C(11) \rightarrow C(12) \rightarrow C(13) \rightarrow C(14) \rightarrow C(15) \rightarrow					
C(20)-H(20A) \cdots Cg(2)	2.93	3.431(9)	1-x,2-y,-z	11.27	113
Ring(1):C(28) \rightarrow C(29) \rightarrow C(30) \rightarrow C(31) \rightarrow C(32) \rightarrow C(33) \rightarrow					

Table S6 Energy levels of 1-3 calculated from CV results

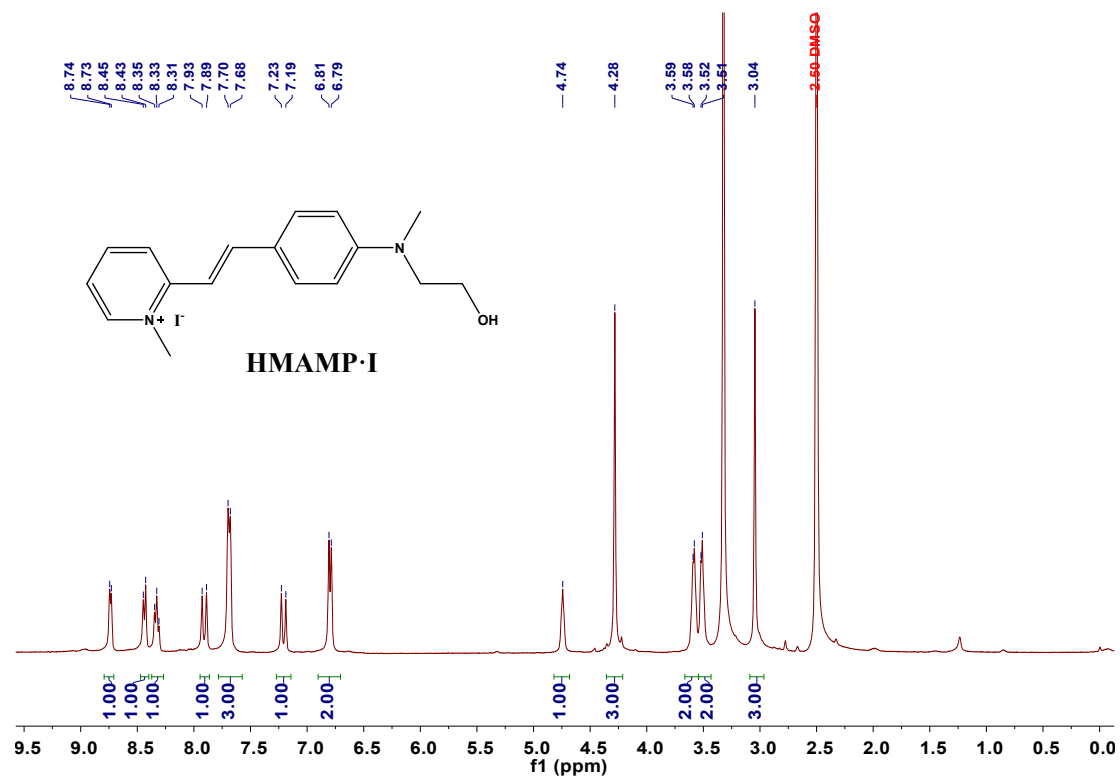
Compound	E _{ox} onset (V)	E _{red} onset (V)	E _{HOMO} (eV)	E _{LUMO} (eV)	E _g (eV)
1	0.67	-1.37	-5.35	-3.07	2.28
2	1.07	-1.16	-5.75	-3.28	2.47
3	1.94	-1.13	-6.62	-3.31	3.31



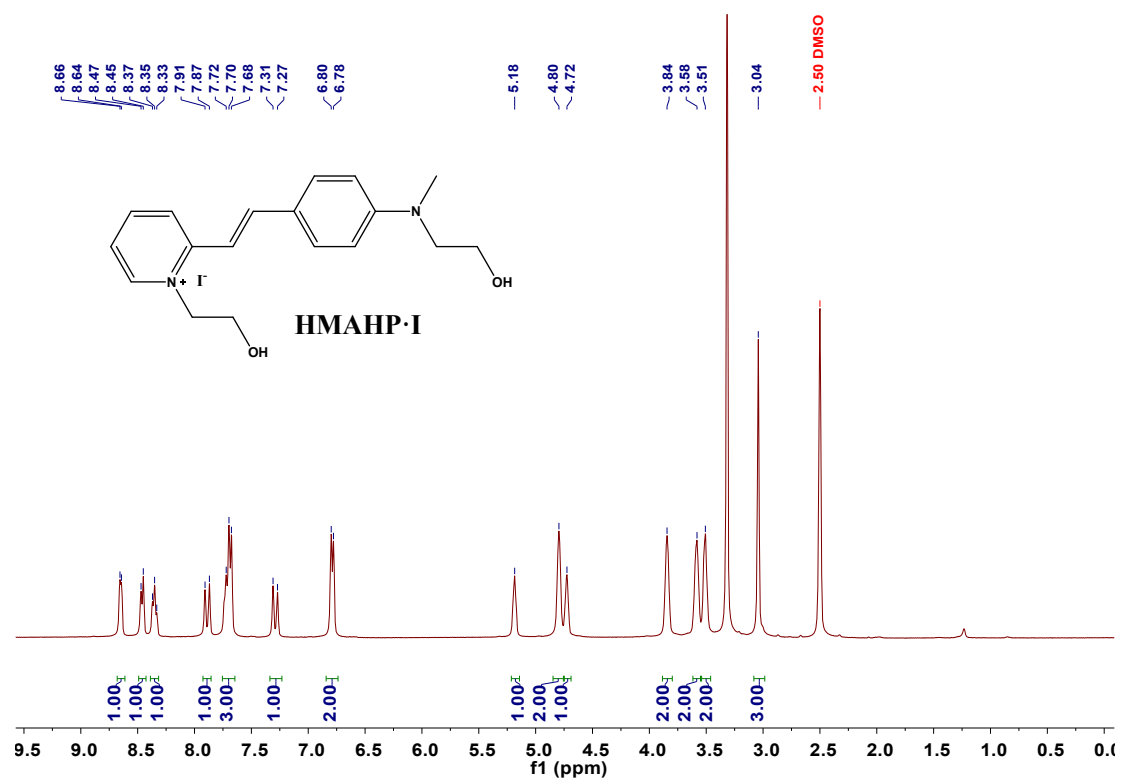
Scheme S1 The preparing process of ITO/active layer/PMMA/Ag memory devices



(a)



(b)



(c)

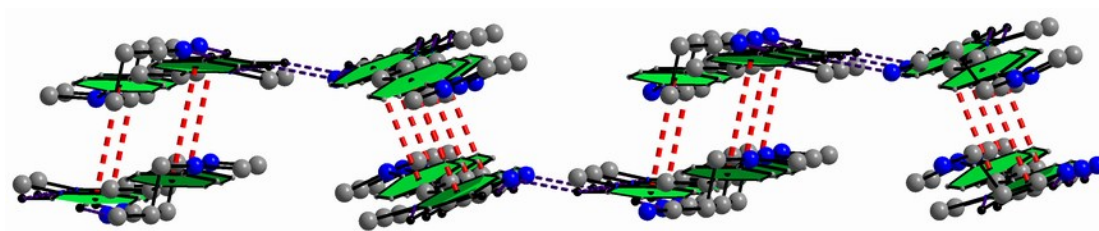
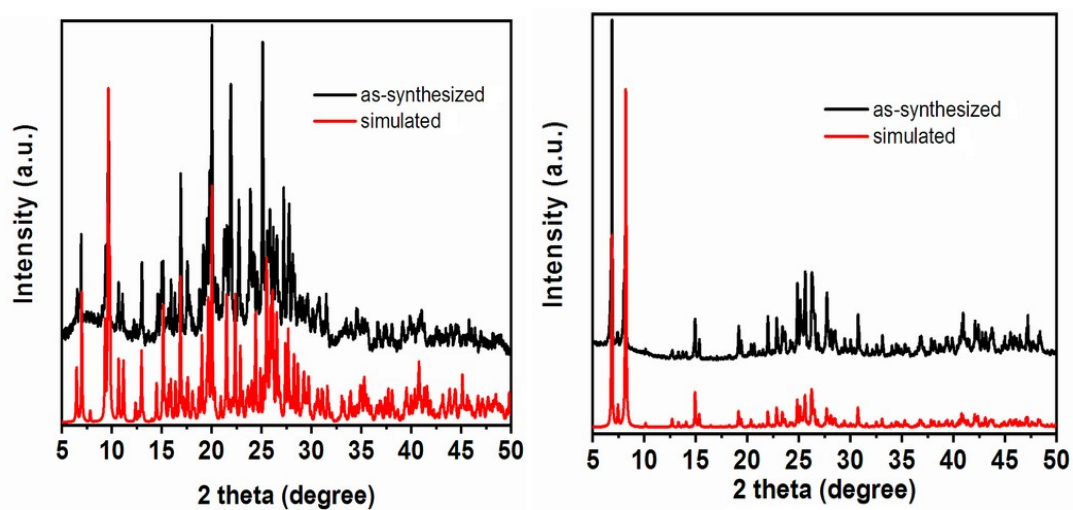
Fig. S1 ¹H NMR spectra of CMAMP-I (a), HMAMP-I (b) and HMAHP-I (c)

Fig. S2 The 2-D cationic layer of 1 (hydrogen atoms without involved in hydrogen bonds were omitted for clarity)



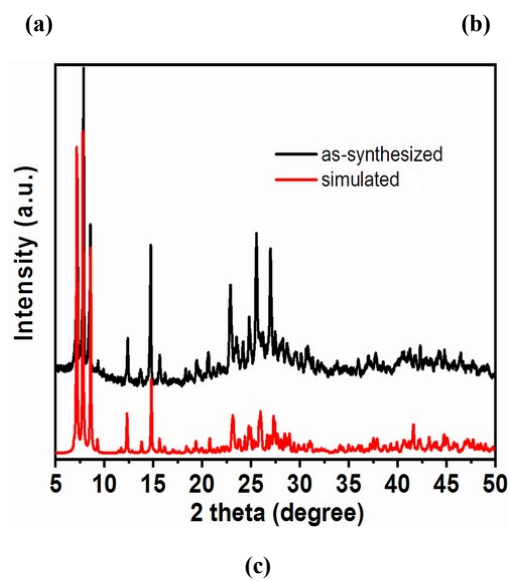


Fig. S3 XRD patterns of 1 (a), 2 (b) and 3 (c)

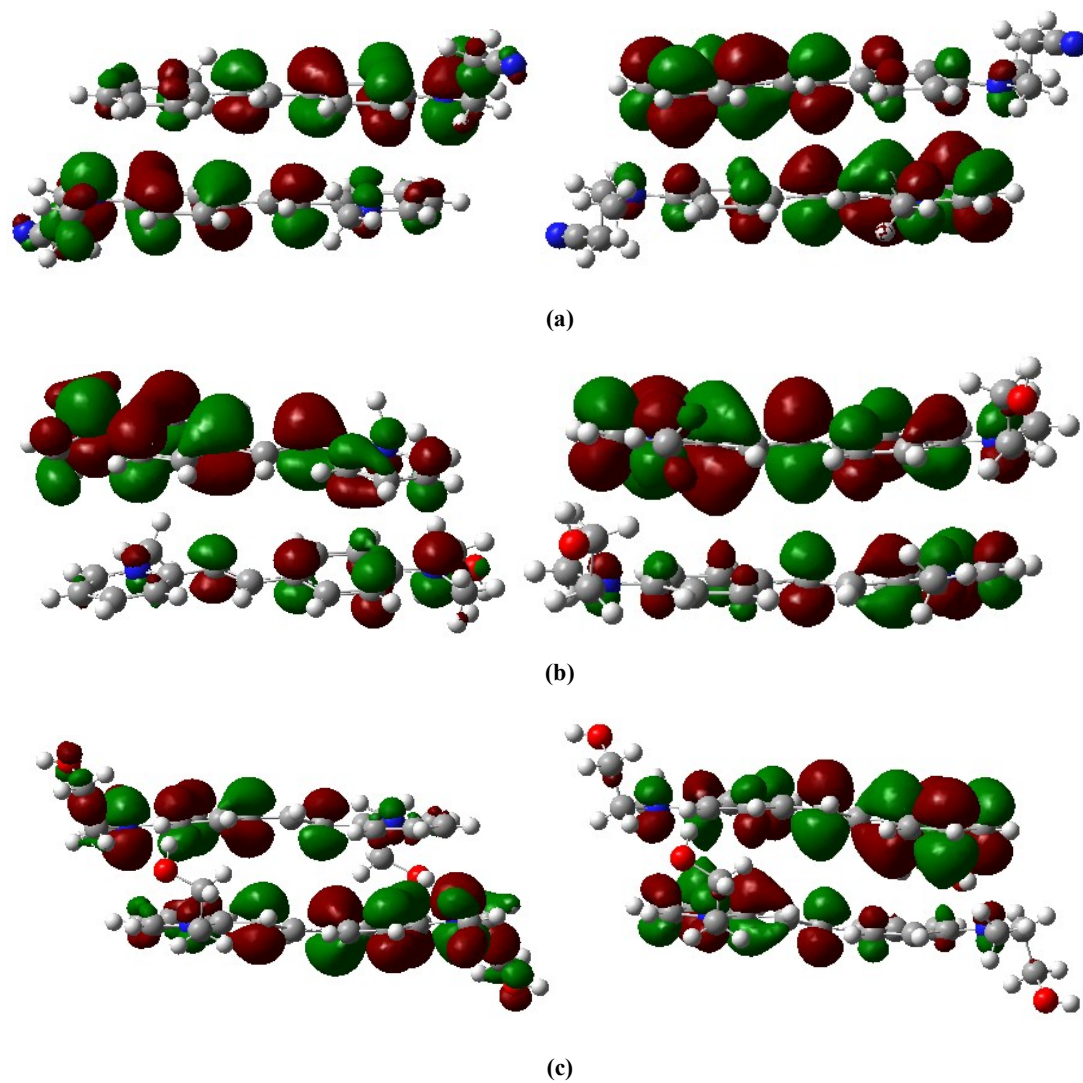


Fig. S4 HOMO (left) and LUMO (right) of CMAMP⁺ dimer in 1 (a), HMAMP⁺ dimer in 2 (b) and HMAHP⁺ dimer in 3 (c)

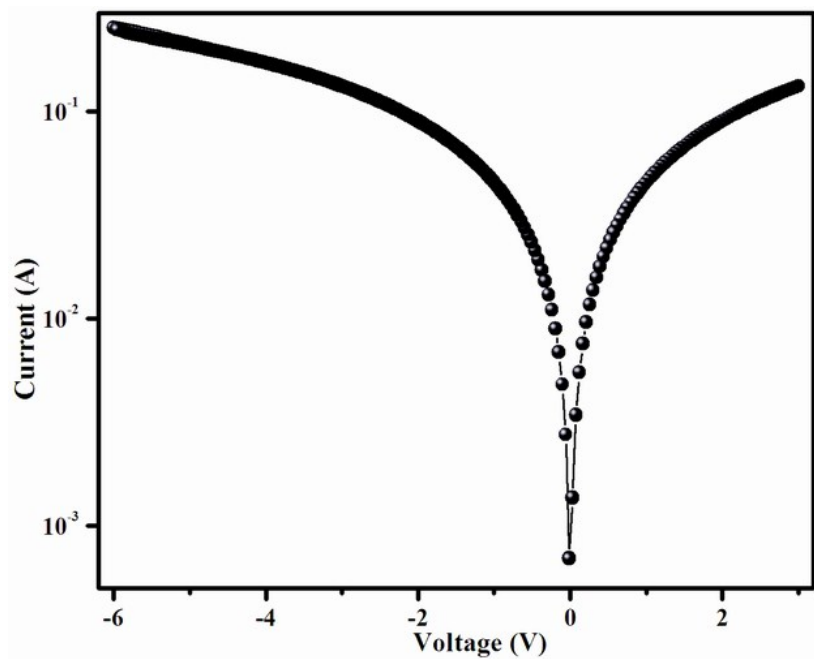


Fig. S5. *I-V* characteristics curves of ITO/hybrid 3/Ag device

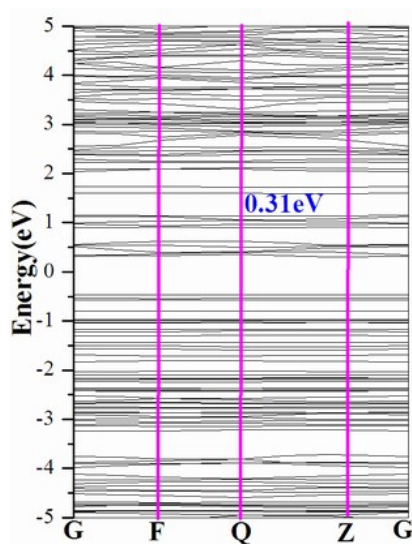
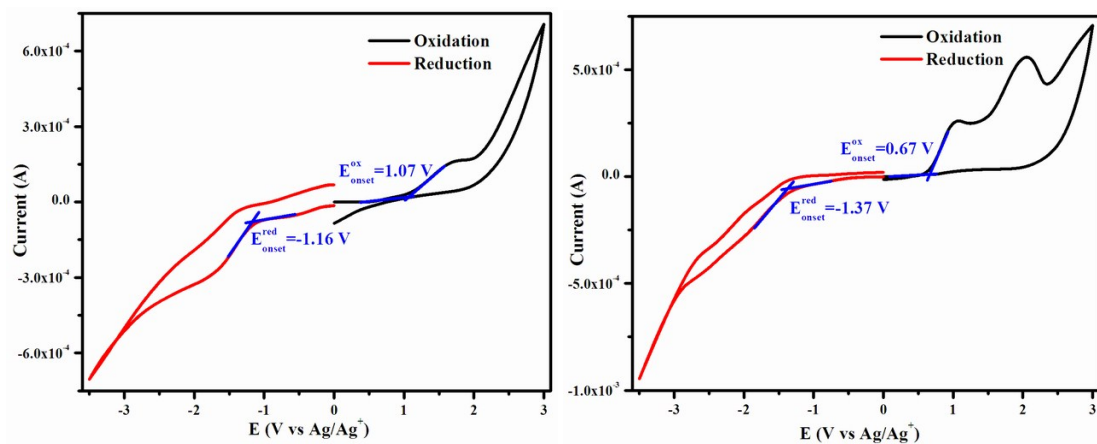


Fig. S6 Band structure of 1



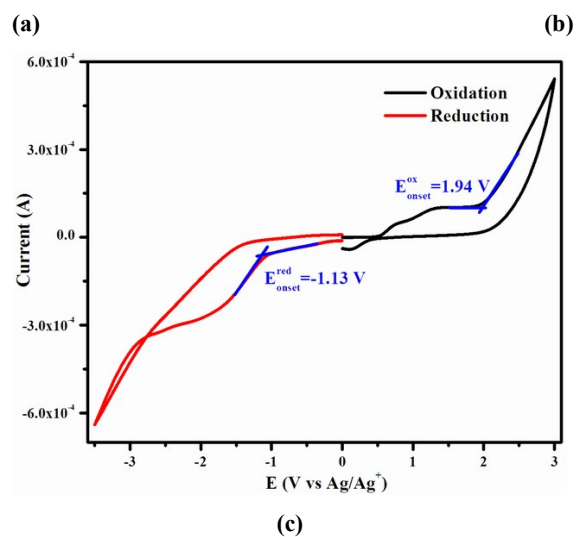


Fig. S7 CV measurements on 1 (a), 2 (b) and 3 (c)

References

1. Frisch, M. J.; Trucks, G. W.; Schlegel, H. B.; et al. Gaussian 09, Revision A01, Gaussian, Inc., Wallingford, CT, 2009.